A Broadband Absorbing Boundary Condition for the FDTD Modeling of Circular Waveguides

Thomas G. Jurgens
Fermi National Accelerator Laboratory
P.O. Box 500, Batavia, Illinois 60510

Abstract— **This paper outlines Berenger's Perfectly Matched Layer absorbing boundary condition applied to the Finite Difference Time Domain modeling of circular waveguides. The model employs a cylindrical body of revolution coordinate system.**

I. Introduction

THE Perfectly Matched Layer (PML) theory developed by Berenger [1] is a major advance in the state of the art of absorbing boundary conditions (ABC) for finite difference time domain (FDTD) methods. Subsequent works have applied the PML theory to three dimensional scattering on cartesian grids [2] and the termination of cartesian meshed waveguides [3]. These papers reported reflection coefficients of better than -70 dB. It is the intent of this work to extend the PML theory to the Body of Revolution (BOR) FDTD modeling of circular waveguides.

The first section provides a background for the BOR-FDTD modeling. The BOR-PML set of relationships are presented next. Finally, modeling results are shown for modes propagating in circular waveguides.

II. BOR-FDTD Background

In the field of particle accelerator design evacuated circular waveguides are commonly used as beam pipes. The beam usually consists of bunches of charged particles. The pipes provide a means of transporting the beam to and through various beamline elements. When a beam bunch passes through these elements, electromagnetic fields may be excited in them. These fields are called wake fields. Succeeding bunches are affected by the wake field, which can lead to beam instability and breakup. Body of revolution FDTD codes have been used for many years to model wake field phenomena in particle accelerators [4] [5] [6] [7] [8]. Proper modeling requires that any modes excited in beam elements and capable of propagating along the beam pipe be absorbed at the numerical grid boundary. The PML method is a broadband ABC superior to those presently in use.

The BOR-FDTD algorithm description starts with Maxwell's time dependent curl equations. Note that a term representing magnetic conductivity is been included here.

$$\nabla \times \vec{H} = \epsilon \frac{\partial \vec{E}}{\partial t} + \sigma \vec{E} \tag{1}$$

$$\nabla \times \vec{E} = -\mu \frac{\partial \vec{H}}{\partial t} + \sigma^* \vec{H} \tag{2}$$

Next, the fields are assumed to have a harmonic azimuthal field dependence.

$$\vec{E} = \sum_{m=0}^{\infty} \vec{e}_u \cos m\phi + \vec{e}_v \sin m\phi \tag{3}$$

$$\vec{H} = \sum_{m=0}^{\infty} \vec{h}_u \cos m\phi + \vec{h}_v \sin m\phi \tag{4}$$

Here $\vec{E}$ and $\vec{H}$ depend on r, ϕ, z and t while $\vec{e_u}$, $\vec{e_v}$, $\vec{h_u}$ and $\vec{h_v}$ depend on r, z and t. The variable m is the mode number. Equations (3)-(4) combined with the cylindrical coordinate forms of (1)-(2) result in the following modal description of the fields.

$$\pm \frac{m}{r} \hat{\phi} \times \vec{h}_{v,u} + \nabla \times \vec{h}_{u,v} = \epsilon \frac{\partial}{\partial t} \vec{e}_{u,v} + \sigma \vec{e}_{u,v} \tag{5}$$

$$\pm \frac{m}{r} \hat{\phi} \times \vec{e}_{v,u} + \nabla \times \vec{e}_{u,v} = -\mu \frac{\partial}{\partial t} \vec{h}_{u,v} + \sigma^* \vec{h}_{u,v} \tag{6}$$

The above vector equations can be separated into two independent groups of six scalar equations. These groups represent modes that are azimuthally perpendicular to each other in a cylindrical waveguide. For the present investigation only one group is needed. It is listed here for later comparison to the PML forms.

CH3577-4/95/0000-0035$01.00 © 1995 IEEE

$$\epsilon\frac{\partial}{\partial t}e_r + \sigma e_r = -\frac{\partial}{\partial z}h_\phi - \frac{m}{r}h_z \quad (7)$$

$$\epsilon\frac{\partial}{\partial t}e_\phi + \sigma e_\phi = \frac{\partial}{\partial z}h_r - \frac{\partial}{\partial r}h_z \quad (8)$$

$$\epsilon\frac{\partial}{\partial t}e_z + \sigma e_z = \frac{1}{r}\frac{\partial}{\partial r}(r\,h_\phi) + \frac{m}{r}h_r \quad (9)$$

$$\mu\frac{\partial}{\partial t}h_r + \sigma^* h_r = \frac{\partial}{\partial z}e_\phi - \frac{m}{r}e_z \quad (10)$$

$$\mu\frac{\partial}{\partial t}h_\phi + \sigma^* h_\phi = -\frac{\partial}{\partial z}e_r + \frac{\partial}{\partial r}e_z \quad (11)$$

$$\mu\frac{\partial}{\partial t}h_z + \sigma^* h_z = -\frac{1}{r}\frac{\partial}{\partial r}(r\,e_\phi) + \frac{m}{r}e_r \quad (12)$$

This set of equations provides a means to numerically analyze structures that are symmetric about an axis. Finite differencing them results in a two dimensional algorithm which computes the fields for a given mode number (m). Non-symmetrical source distributions are modeled by representing the source as a sum of its azimuthal moments and solving for their field distributions one mode at a time.

III. The PML Methodology

The PML method separately computes the contribution for each of the two terms of the curl operator. Thus (7)-(12) become a set of twelve equations. In the equations below the first subscript refers to the field component's coordinate direction, while the second subscript indicates which term of the curl operator contributes to the field component's temporal update.

$$\epsilon\frac{\partial}{\partial t}e_{rz} + \sigma_z e_{rz} = -\frac{\partial}{\partial z}(h_{\phi z} + h_{\phi r}) \quad (13)$$

$$\epsilon\frac{\partial}{\partial t}e_{r\phi} + \sigma_\phi e_{r\phi} = -\frac{m}{r}(h_{zr} + h_{z\phi}) \quad (14)$$

$$\epsilon\frac{\partial}{\partial t}e_{\phi z} + \sigma_z e_{\phi z} = \frac{\partial}{\partial z}(h_{rz} + h_{r\phi}) \quad (15)$$

$$\epsilon\frac{\partial}{\partial t}e_{\phi r} + \sigma_r e_{\phi r} = -\frac{\partial}{\partial r}(h_{zr} + h_{z\phi}) \quad (16)$$

$$\epsilon\frac{\partial}{\partial t}e_{zr} + \sigma_r e_{zr} = \frac{1}{r}\frac{\partial}{\partial r}(r(h_{\phi z} + h_{\phi r})) \quad (17)$$

$$\epsilon\frac{\partial}{\partial t}e_{z\phi} + \sigma_\phi e_{z\phi} = \frac{m}{r}(h_{rz} + h_{r\phi}) \quad (18)$$

$$\mu\frac{\partial}{\partial t}h_{rz} + \sigma_z^* h_{rz} = \frac{\partial}{\partial z}(e_{\phi z} + e_{\phi r}) \quad (19)$$

$$\mu\frac{\partial}{\partial t}h_{r\phi} + \sigma_\phi^* h_{r\phi} = -\frac{m}{r}(e_{zr} + e_{z\phi}) \quad (20)$$

$$\mu\frac{\partial}{\partial t}h_{\phi z} + \sigma_z^* h_{\phi z} = -\frac{\partial}{\partial z}(e_{rz} + e_{r\phi}) \quad (21)$$

$$\mu\frac{\partial}{\partial t}h_{\phi r} + \sigma_r^* h_{\phi r} = \frac{\partial}{\partial r}(e_{zr} + e_{z\phi}) \quad (22)$$

$$\mu\frac{\partial}{\partial t}h_{zr} + \sigma_r^* h_{zr} = -\frac{1}{r}\frac{\partial}{\partial r}(r(e_{\phi z} + e_{\phi r})) \quad (23)$$

$$\mu\frac{\partial}{\partial t}h_{z\phi} + \sigma_\phi^* h_{z\phi} = \frac{m}{r}(e_{rz} + e_{r\phi}) \quad (24)$$

The PML method requires that the ratio of the electric conductivity to the permittivity equals the ratio of the magnetic field conductivity to the permeability across the interface of the PML and the interior of the grid.

$$\sigma/\epsilon = \sigma^*/\mu \quad (25)$$

The waveguide under consideration is empty and has terminating planes perpendicular to the z-axis. Satisfaction of (25) requires the following conductivities to be set to zero:

$$\sigma_r = \sigma_r^* = \sigma_\phi = \sigma_\phi^* = 0 \quad (26)$$

Inside the PML a parabolic conductivity profile is used for σ_z and σ_z^*.

$$\sigma(z') = \sigma_{\max}(z'/\delta)^2 \quad (27)$$

The maximum conductivity, $\sigma_{\max}$ is 10 S/m and z' is measured from the vacuum boundary of the PML. Exponential time stepping [1] [9] is utilized for the calculation of the difference equations containing σ_z and σ_z^*. The PML thickness, δ, is 20 mm.

IV. Results

The object modeled is a perfect electrically conducting (PEC) circular waveguide, as illustrated in Fig. 1. The guide radius is 26 mm. PEC material terminates the waveguide at $z = z_{\max}$. The PML is located immediately to the left of the PEC termination. The PML thickness, δ is $20\,\Delta z$ where $\Delta z = 1$ mm, the spatial increment in the z-direction. The modes are excited at $z = z_{\min}$ and allowed to propagate into the PML.

The first example is a TM01 excitation by a 6 GHz carrier modulated by a gaussian pulse. The pulse has a full width half maximum (FWHM) of 682 ps, it frequency spectrum is shown in Fig. 2. The cutoff frequency of the TM01 mode is 4.413 GHz. Fig. 3 shows the spectrum of the reflection coefficient at the PML/vacuum interface. Over the illustrated 6 GHz bandwidth, the reflection coefficient due to the PML termination varies between -85 and -120 dB. Note that the PML is effective at matching the evanescent fields below the 4.413 GHz cutoff frequency.

The second example is a TE11 excitation with a gaussian pulse modulating a 4.4 GHz carrier. The

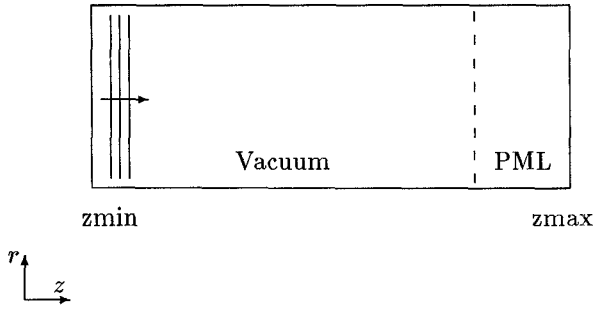

Fig. 1. FDTD excitation of a circular waveguide terminated with PML media

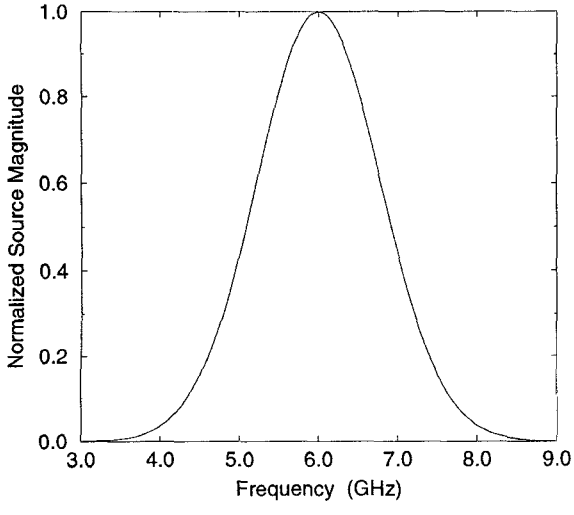

Fig. 2. Spectrum of the TM01 gaussian pulse

pulse has a FWHM of 682 ps, it frequency spectrum is shown in Fig. 4. sinusoidal waveform. The guide cutoff frequency for this mode is 3.379 GHz. Fig. 5 shows the spectrum of the reflection coefficient at the PML/vacuum interface over a 6 GHz bandwidth. The reflection coefficient varies between -95 dB and -105 dB. Once again, the PML is able to absorb the evanescent fields below 3.379 GHz.

V. Conclusion

The PML ABC has been demonstrated for PEC circular waveguides modeled with a BOR-FDTD algorithm. Boundary reflections were found to be less than -85 db, which compares favorably with previous studies. Future investigations will include applying the PML method to dielectric waveguides and open structures.

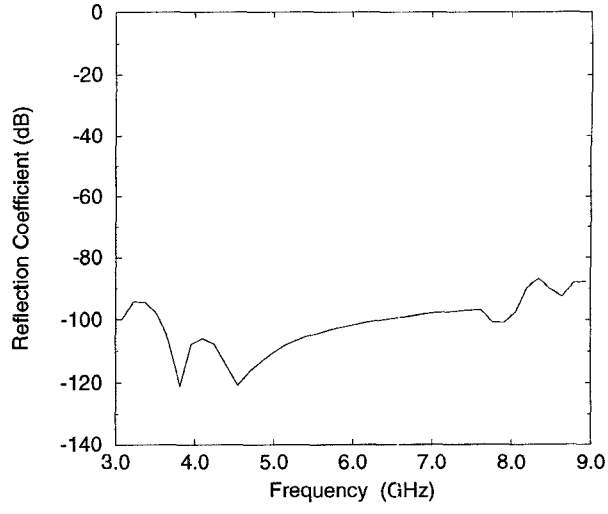

Fig. 3. Reflection coefficient for the TM01 pulse at the vacuum/PML interface

References

[1] J.-P. Berenger, "A perfectly matched layer for the absorption of electromagnetic waves", *Journal of Computational Physics*, vol. 114, pp. 185–200, Oct. 1994.

[2] D. S. Katz, E. T. Thiele, and A. Taflove, "Validation and extension to three dimensions of the Berenger PML absorbing boundary condition for FDTD meshes", *IEEE Microwave and Guided Wave Lett.*, vol. 4, pp. 268–270, Aug. 1994.

[3] C. E. Reuter, R. M. Joseph, E. T. Thiele, D. S. Katz, and A. Taflove, "Ultrawideband absorbing boundary condition for termination of waveguiding structures in FDTD simulations", *IEEE Microwave and Guided Wave Lett.*, vol. 4, pp. 344–346, Oct. 1994.

[4] G. Aharonian, R. Meller, and R. H. Siemann, "Transverse wakefield calculations", *Nuclear Instruments and Methods*, vol. 212, pp. 23–35, 1983.

[5] T. Weiland, "Transverse beam cavity interaction. Part I: short range forces", *Nuclear Instruments and Methods*, vol. 212, pp. 13–21, 1983.

[6] Y. H. Chin, "User's guide for ABCI Version 8.7", Tech. Rep. LBL-35258, Lawrence Berkley Laboratory, 1994.

[7] C. C. Shang and J. F. DeFord, "Modified Yee solutions in the AMOS wakefield code", in *Proceedings of the 1990 Linear Accelerator Conference*, Albuquerque, NM, Sept. 1990, pp. 378–380.

[8] T. G. Jurgens, G. W. Saewert, and F. A. Harfoush, "Xwake 1.0: A new tool for wakefield and impedance calculations", in *Proceedings of the 4th European Particle Accelerator Conference*, London, UK, June 1994.

[9] R. Holland, "Finite difference time domain (FDTD) analysis of magnetic diffusion", *IEEE Trans. Electromagn. Compat.*, vol. 36, pp. 32–39, Feb. 1994.

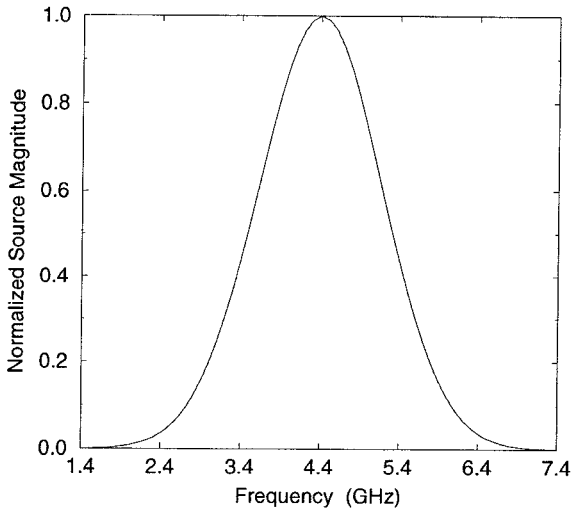

Fig. 4. Spectrum of the TE11 gaussian pulse

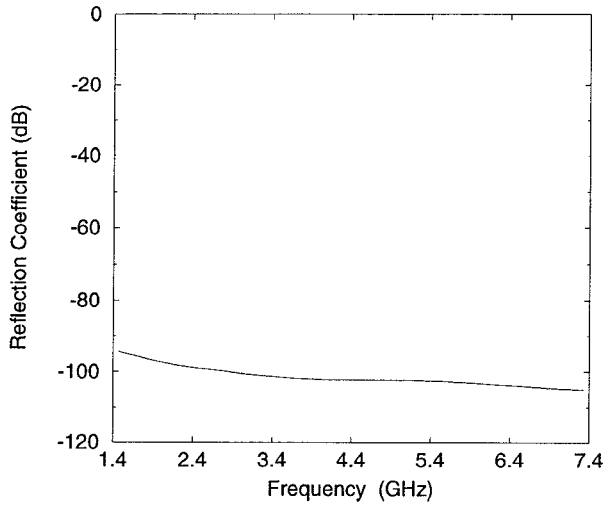

Fig. 5. Reflection coefficient for the TE11 pulse at the vacuum/PML interface